

Hot-electron distribution functions in a subpicosecond laser interaction with solid targets of varying initial gradient scale lengths

S. Bastiani,* P. Audebert, J. P. Geindre, Th. Schlegel, and J. C. Gauthier

Laboratoire pour l'Utilisation des Lasers Intenses, UMR No. 7605 CNRS, Ecole Polytechnique, CEA, Université Paris VI, Ecole Polytechnique, 91128 Palaiseau, France

C. Quoiix, G. Hamoniaux, G. Grillon, and A. Antonetti

Laboratoire d'Optique Appliquée, URA No. 1406 CNRS, Batterie de l'Yvette, 91761 Palaiseau, France

(Received 20 January 1999)

We have studied the distribution function of the hot electrons produced during the interaction of a 120-fs, 60-mJ, 800-nm wavelength and a *p*-polarized laser pulse with bilayered Al/Fe targets. The main pulse interacts with a preformed plasma, obtained with a controlled prepulse, whose density gradient scale length has been measured. The electron distribution function is characterized by means of the $K\alpha$ emission of the two materials of the target as a function of the Al-layer thickness. The low-energy region (<50 keV) of the hot-electron distribution function shows no dependency in shape on the gradient scale length, but only a variation in the total number of the generated electrons. The comparison between the experimental results and the particle-in-cell and Monte Carlo calculations of the electron distribution function and the $K\alpha$ emission is gratifying. [S1063-651X(99)07209-8]

PACS number(s): 52.50.Jm, 52.70.La, 52.65.Rr

High-intensity, subpicosecond-pulsed lasers have opened a new field of research in the laser-matter interaction [1,2] and the created plasmas have attracted great attention as bright and ultrashort x-ray sources [3–7]. In this kind of interaction, the laser energy is absorbed within the laser skin depth and gives rise to a plasma whose lifetime is comparable to the laser-pulse duration and whose spatial scale length is of the order of a few tens of nanometers. This thermal plasma has several hundred electronvolts electron temperature and approaches solid density. Due to the high electron density and steep density and temperature gradients, the thermal conduction into the bulk of the target and the hydrodynamic expansion produce a rapid quenching of x-ray emission.

Beside collisional absorption, several nonlinear absorption mechanisms have been shown to contribute to the overall laser energy deposition. Among them, the most efficient are the resonant absorption [8], the “vacuum heating” [9], and forward-scattering instabilities in the strongly-driven regime [10]. These nonlinear mechanisms produce hot electrons, which are interesting to study for essentially two reasons. First, it allows us to get more insight on the absorption processes present during the interaction. Second, the hot electrons are responsible, if their energy is not too high, of the x-ray $K\alpha$ -line emission. This emission is generated in the solid material by inner-shell ionization from fast electrons that penetrate in the target bulk, so its intensity and time duration depend on the electron characteristics: their number and their energy. The nonthermal emission has also been shown to be very short because, in principle, hot electrons are produced only during the laser pulse. For light elements

like aluminum, the K -shell ionization cross section is maximum for electrons' energies of a few keV, so this line can be utilized as a diagnostic for “not-so-fast” electron production.

Many experimental works have shown that the x-ray yield is increased when the laser interacts not with the surface of the solid target but with a preformed plasma originating from irradiation of the solid surface with an earlier pulse or with amplified spontaneous emission from the laser [6,11–13]. In an earlier paper [14], we reported a systematic study of the influence of a preplasma on the absorption coefficient and on the characteristics of hot electrons which *escape* the plasma toward the vacuum. We change the electron-density gradient scale length by varying the temporal separation between the main laser pulse and a prepulse of the same duration but with 1% of the intensity of the main interacting pulse. Doing this, we have explored the highly complex transition between steplike gradient absorption and resonant absorption. In the present experiment, we utilize the same procedure to characterize the hot electrons *penetrating* in the target, which are responsible for the $K\alpha$ production. To characterize the electron distribution function, we use bilayered targets, consisting of different film thicknesses of aluminum deposited on an iron substrate. By measuring the $K\alpha$ yield of both materials as a function of the Al film thickness, we get an insight into the characteristics of the hot electrons generated during the interaction [15].

The experiments have been carried out using the chirped pulse amplification (CPA) Titane:Sapphire laser system developed at the Laboratoire d'Optique Appliquée in Palaiseau [16]. This laser is capable of delivering a 120-fs duration, 60-mJ energy, 800-nm wavelength, and 10-Hz repetition rate pulses. The laser intensity contrast ratio is measured to be 10^{-8} , at 2 ps before the main pulse, by third-order autocorrelation techniques. The beam is focused with a 40-cm ($f/16$) focal length MgF_2 lens, at an incidence angle of 45° .

*Present address: Commissariat à l'Energie Atomique, DRECAM/SRSIM, Bâtiment 462, Center d'Etudes de Saclay, 91191 Gif-sur-Yvette Cedex, France.

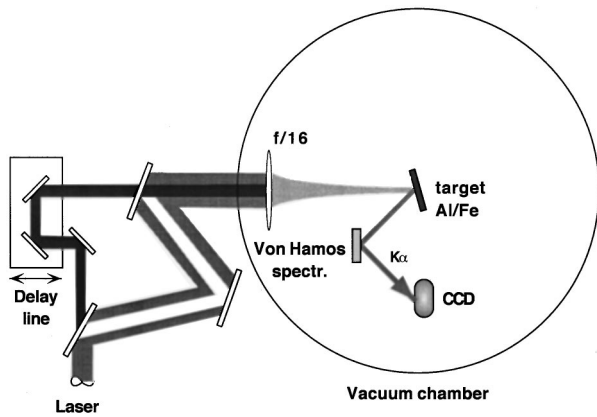


FIG. 1. Sketch of the experimental apparatus, showing the main pulse, prepulse optical arrangement, and the x-ray spectrograph.

The targets are massive Fe covered by a vacuum-deposited Al coating, with thicknesses varying from 60 to 4000 nm. In Fig. 1 is sketched the experimental setup and, in particular, the arrangement utilized for the controlled prepulse production [14]. Typically, this system gives intensities on the target of 4×10^{16} W/cm² for the main pulse and 4×10^{14} W/cm² for the prepulse, with focal spots of a 24- μ m diameter (at $1/e^2$ of maximum intensity) for the main pulse and 140 μ m (first Airy disk diameter) for the prepulse. Targets were mounted on a X-Y-Z motorized translational system to expose a fresh surface of the target to each laser shot.

The $K\alpha$ emission is analyzed by means of two Von Hamos spectrographs built with an ammonium dihydrogen phosphate crystal ($2d = 10.648$ Å) of 22-cm curvature radius and with a Quartz crystal ($2d = 2.451$ Å) of a 22.5-cm curvature radius. The geometry of the spectrographs has been carefully chosen to allow the simultaneous measurement of both spectra at each laser shot. The spectra were collected on a cooled (-40 °C) x-ray sensitive charge-coupled-device (CCD) camera, at an angle of 45° with respect to the target normal. To decrease the background of the CCD image (which was attributed to high-energy electron-induced x-ray fluorescence) the entire interaction region was shielded with a lead enclosure.

We measure the Al and Fe $K\alpha$ yield as a function of the deposited Al thickness and for various prepulse-to-main pulse delays. This is equivalent to analyze the effect of an initial gradient density scale length on the absorption mechanism and the fast electrons production. Obviously, this analysis is fully exploitable only if one is able to find a link between the pulse delay and the gradient scale length of the resulting preplasma. Using spectral interferometry [17], we have measured the gradient scale length of the preformed plasma as a function of time. In Fig. 2, we show the measured gradient scale length of a silicon plasma (whose expansion dynamics is nearly identical to that of the aluminum), compared with an isotherm expansion model [18]. In the following, these results are used to “translate” the experimental parameter (the delay between the pulses) into the relevant physical quantity (the density gradient scale length).

The experimental data have been compared with the results of a Monte Carlo code used as a post processor for the results of a particle-in-cell (PIC) code. The PIC code is the $1\frac{1}{2}$ -D relativistic code EUTERPE [19], which uses the “boost-

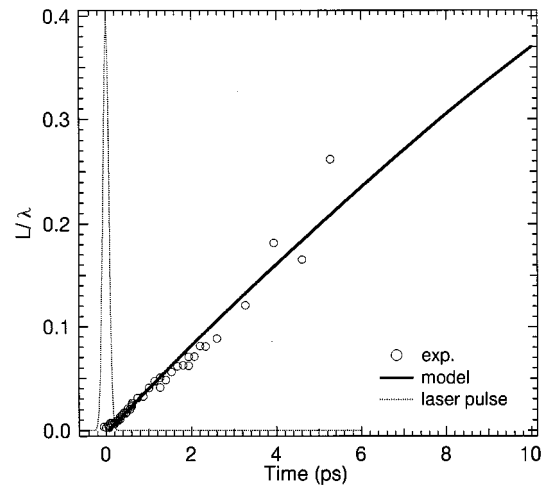


FIG. 2. Experimental measurement of the electron-density gradient scale length in silicon as a function of the expansion time after the prepulse (open circles). The solid line shows the isothermal model with $T_e = 50$ eV and an average charge of $Z^* = 5$. The dotted line represents the temporal shape of the laser prepulse.

frame” transformation [20] to account for oblique laser incidence. The simulations have been performed with an initial linear-density profile of various gradient scale lengths, ranging from $L/\lambda = 0.001$ to $L/\lambda = 0.7$. The other parameters are as follows: maximum density $9.5n_c$, initial temperatures 600 eV for electrons and 100 eV for ions, incidence angle 45° , mobile ions with $M_i/Zm_e = 3600$, and 1.4×10^5 particles. The laser pulse is Gaussian, of 120-fs full width at half maximum duration. The boundary conditions for particles reaching the walls of the simulation box are reflection for all the ions and for the electrons that escape toward the vacuum and reinjection with the initial distribution at 600 eV for the electrons escaping the solid bulk. The Monte Carlo code follows the three-dimensional trajectories of each electron (in a group of monoenergetic electrons) interacting with the bilayered target through elastic and inelastic scattering. The former is treated via the screened Rutherford cross section and the latter via the Bethe stopping-power cross section. The code takes into account the opacity of the material between the emission region and the detector. By weighting the results obtained at several electron energies with each energy component of the electron distribution function resulting from the PIC code, we can calculate the overall $K\alpha$ emission.

In Fig. 3 we report the Al $K\alpha$ and Fe $K\alpha$ lines’ intensities as a function of the Al layer thickness and for various prepulse main-pulse delays. The experimental data have been compared with the results of PIC simulations, “post-processed” with the Monte Carlo code. Each point is the result of an average over ten laser shots. The Al $K\alpha$ yield shows a plateau for the highest values of film thickness, which indicates the maximum penetration depth of the electrons: no more emission is generated in the deeper regions. Conversely, the Fe $K\alpha$ yield shows a similar plateau for the smallest Al film thickness. From the experimental results, it is immediately apparent that the presence of a preplasma allows a gain of a factor of three in the $K\alpha$ emission.

Due to the lack of absolute calibration of the Von Hamos spectrographs, we do not have a quantitative measurement of

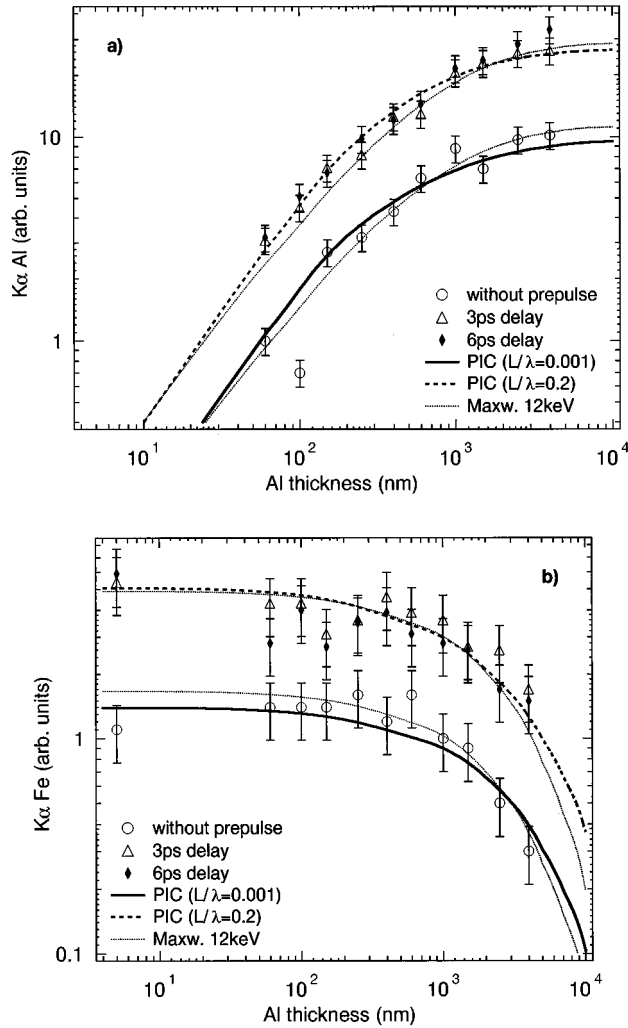


FIG. 3. $K\alpha$ emission of Al [Fig. 3(a)] and Fe [Fig. 3(b)] as a function of the Al layer thickness and for various prepulse, main pulse delays. The solid and the dashed lines are the calculated $K\alpha$ emissions obtained from the PIC distribution functions corresponding to different initial gradient scale lengths. The dotted line is the $K\alpha$ emission calculated from a 12-keV Maxwellian distribution function.

the $K\alpha$ photon number, so we cannot infer the conversion efficiency of the laser energy into suprathermal electrons. Consequently, to allow the comparison with the experimental data, the calculated curves have been scaled with two arbitrary factors (one for each crystal) to account for the unknown crystal reflectivities. The comparison with the experimental $K\alpha$ emission is gratifying.

Starting from these results, we can also determine which energy range of the electron distribution function is mainly responsible for the $K\alpha$ emission. We find that 91% of the Al $K\alpha$ emission and 65% of the Fe $K\alpha$ emission is due to electrons with energy lower than 35 keV. We can, therefore, conclude, at least for the Al emission, that the $K\alpha$ source duration is of the same order of the 35-keV electrons stopping time in aluminum, which is about 200 fs. This is confirmed by our recent time-resolved x-ray diffraction experiment, in which the time duration of the laser-induced atom disorder in the sample was of the order of 300 fs [21].

In Fig. 3, we also report the $K\alpha$ emission obtained start-

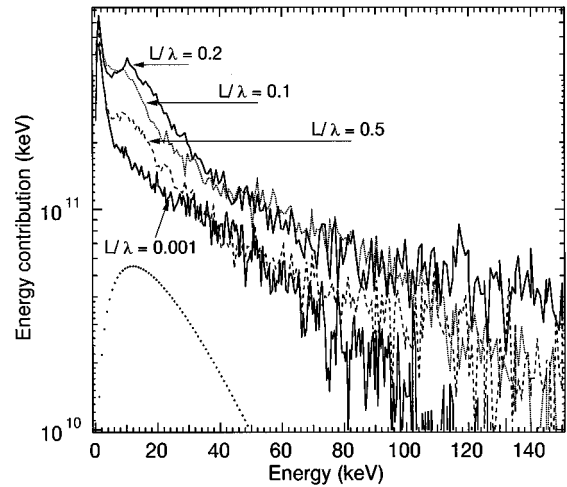


FIG. 4. Product $Ef(E)$ as a function of the electron energy E for various normalized initial gradient scale lengths. The dotted line gives the result for a 12-keV Maxwellian distribution function (not to scale).

ing from a 12-keV Maxwellian electron distribution function. This allows a “compact” description of the electrons and an easier comparison with older results on the hot-electron temperature. Calculations with 10- and 14-keV distributions are compatible with the experimental error bars. Incidentally, we note that the 12-keV “hot-electron” temperature is in excellent agreement with previous results reported in the literature (see Fig. 4 in Ref. [2]). We show in Fig. 4 the energy contribution of each component of the distribution function $f(E)$, i.e., $Ef(E)$. We observe the appearance of two major energy contributions: the first at 600 eV, which represents the thermal electrons, and the second at about 10 keV, the position of which is found to be independent of the value of the density gradient scale length. The energy transported by the electrons is, so to speak, accumulated around 10 keV, which is consistent with a Maxwellian distribution function with a characteristic temperature of 12 keV (see the dotted curve in Fig. 4).

In our earlier paper [14], we have shown the existence of a value of the initial density scale length ($L/\lambda \approx 0.2$) for which we obtained a maximum in the laser energy absorption (65%, against 30% in the case of no prepulse) and, at the same time, a maximum in number and hot temperature of electrons that *escape* the plasma (182 keV, against 19 keV with no prepulse), i.e., a strong modification of the distribution function of these electrons. We already suggested that the electron energy distribution function was highly anisotropic in directions going inward and outward of the target. A further analysis on the outward electron distribution function had shown that these electrons were essentially those that undergo backscattering by the solid and which have enough energy to escape the charge separation barrier in front of the target. The “optimum” value $L/\lambda \approx 0.2$ is in good agreement with the value for maximum absorption predicted by the standard theory of resonance absorption [8].

From the present results, we can conclude that the electron distribution function of the “hot electrons” is essentially made of two components. The first, at low energies

(say, <50 keV, see also Fig. 4), is characterized by a Maxwellian temperature of 12 ± 2 keV. This temperature is independent on the electron-density gradient length with which the laser interacts. However, we must stress again that our study is limited to short scale lengths ($L/\lambda < 0.5$). On the contrary, the electron number is a function of the value of the scale length. This low-energy component is almost entirely responsible for the $K\alpha$ emission. The second component of the electron distribution function, at higher energies, exhibits

a strong dependence on the initial scale length value, for both the “hot-electron” temperature and the number of electrons. A detailed analysis of this high-energy component is the subject of another paper [22].

We gratefully acknowledge the support of the laser staff at Laboratoire d’Optique Appliquée where the experiments were carried out. This work was supported by the European Training and Mobility Contract No. ERBFMRXCT96-0080.

-
- [1] J. C. Gauthier, in *Laser Interaction with Matter*, edited by S. Rose, IOP Conf. Proc. No. 140 (Institute of Physics and Physical Society, Bristol, 1994), p. 1.
- [2] P. Gibbon and E. Förster, *Plasma Phys. Controlled Fusion* **38**, 769 (1996).
- [3] J. F. Pelletier, M. Chaker, and J. C. Kieffer, *Appl. Phys. Lett.* **69**, 2172 (1996).
- [4] J. Workman, A. Maksimchuk, X. Liu, U. Ellenberger, J. S. Coe, X. Y. Chien, and D. Umstadter, *J. Opt. Soc. Am. B* **13**, 125 (1996).
- [5] J. C. Kieffer, M. Chaker, J. P. Matte, H. Pépin, C. Y. Côté, Y. Beaudin, C. Y. Chien, S. Coe, G. Mourou, and O. Peyrusse, *Phys. Fluids B* **5**, 2676 (1993).
- [6] A. Rousse, P. Audebert, J. P. Geindre, F. Fallières, J. C. Gauthier, A. Mysyrowicz, G. Grillon, and A. Antonetti, *Phys. Rev. E* **50**, 2200 (1994).
- [7] J. C. Kieffer, Z. Jiang, A. Ikhlef, and C. Y. Côté, *J. Opt. Soc. Am. B* **13**, 132 (1996).
- [8] W. L. Kruer, *The Physics of Laser Plasma Interactions* (Addison-Wesley, Redwood City, CA, 1988).
- [9] F. Brunel, *Phys. Rev. Lett.* **59**, 52 (1987); *Phys. Fluids* **31**, 2714 (1988).
- [10] D. Gordon *et al.*, *Phys. Rev. Lett.* **80**, 2133 (1998).
- [11] G. A. Kyrala, R. D. Fulton, E. K. Wahlin, L. A. Jones, G. T. Schappert, J. A. Cobble, and A. J. Taylor, *Appl. Phys. Lett.* **60**, 2195 (1992).
- [12] U. Teubner, G. Kühnle, and F. P. Schäfer, *Appl. Phys. B: Photophys. Laser Chem.* **54**, 493 (1992).
- [13] H. Ahn, H. Nakano, T. Nishikawa, and N. Uesugi, *Jpn. J. Appl. Phys., Part 2* **35**, L154 (1996).
- [14] S. Bastiani, A. Rousse, J. P. Geindre, P. Audebert, C. Quoi, G. Hamoniaux, A. Antonetti, and J. C. Gauthier, *Phys. Rev. E* **56**, 7179 (1997).
- [15] J. D. Hares, J. D.ilkenny, M. H. Key, and J. G. Lunney, *Phys. Rev. Lett.* **42**, 1216 (1979).
- [16] C. Le Blanc, G. Grillon, J. P. Chambaret, A. Migus, and A. Antonetti, *Opt. Lett.* **18**, 140 (1993).
- [17] J. P. Geindre, P. Audebert, A. Rousse, F. Fallières, J. C. Gauthier, A. Mysyrowicz, A. Dos Santos, G. Hamoniaux, and A. Antonetti, *Opt. Lett.* **19**, 1997 (1995).
- [18] M. D. Rosen, *Proc. SPIE* **1229**, 160 (1990).
- [19] G. Bonnaud and G. Reisse, *Nucl. Fusion* **26**, 633 (1986).
- [20] A. Bourdier, *Phys. Fluids* **26**, 1804 (1983).
- [21] C. Rischel, A. Rousse, I. Uschmann, P. A. Albouy, J. P. Geindre, P. Audebert, J. C. Gauthier, E. Förster, J. L. Martin, and A. Antonetti, *Nature (London)* **390**, 490 (1997).
- [22] Th. Schlegel, S. Bastiani, L. Grémillet, J. P. Geindre, P. Audebert, J. C. Gauthier, E. Lefebvre, G. Bonnaud, and J. Delettrez, *Phys. Rev. E* **60**, 2209 (1999).